



Published in final edited form as:

*Exp Dermatol.* 2016 May ; 25(5): 362–367. doi:10.1111/exd.12932.

## Longitudinal *in vivo* tracking of adverse effects following topical steroid treatment

Andrew J. Bower<sup>1,2</sup>, Zane Arp<sup>3</sup>, Youbo Zhao<sup>1</sup>, Joanne Li<sup>4</sup>, Eric J. Chaney<sup>1</sup>, Marina Marjanovic<sup>1</sup>, Angela Hughes-Earle<sup>3</sup>, and Stephen A. Boppart<sup>\*,1,2,4,5</sup>

<sup>1</sup>Beckman Institute for Advanced Science and Technology, University of Illinois at Urbana-Champaign, Urbana, IL

<sup>2</sup>Department of Electrical and Computer Engineering, University of Illinois at Urbana-Champaign, Urbana, IL

<sup>3</sup>GlaxoSmithKline, King of Prussia, PA

<sup>4</sup>Department of Bioengineering, University of Illinois at Urbana-Champaign, Urbana, IL

<sup>5</sup>Department of Internal Medicine, University of Illinois at Urbana-Champaign, Urbana, IL

### Abstract

Topical steroids are known for their anti-inflammatory properties and are commonly prescribed to treat many adverse skin conditions such as eczema and psoriasis. While these treatments are known to be effective, adverse effects including skin atrophy are common. In this study, the progression of these effects is investigated in an *in vivo* mouse model using multimodal optical microscopy. Utilizing a system capable of performing two-photon excitation fluorescence microscopy (TPEF) of reduced nicotinamide adenine dinucleotide (NADH) to visualize the epidermal cell layers and second harmonic generation (SHG) microscopy to identify collagen in the dermis, these processes can be studied at the cellular level. Fluorescence lifetime imaging microscopy (FLIM) is also utilized to image intracellular NADH levels to obtain molecular information regarding metabolic activity following steroid treatment. In this study, fluticasone propionate (FP) treated, mometasone furoate (MF) treated, and untreated animals were imaged longitudinally using a custom-built multimodal optical microscope. Prolonged steroid treatment over the course of 21 days is shown to result in a significant increase in mean fluorescence lifetime of NADH, suggesting a faster rate of maturation of epidermal keratinocytes. Alterations to collagen organization and the structural microenvironment are also observed. These results give insight into the structural and biochemical processes of skin atrophy associated with prolonged steroid treatment.

### Keywords

Fluorescence Lifetime Imaging Microscopy; Multiphoton Microscopy; Second Harmonic Generation Microscopy; Topical Steroids; Skin Atrophy

\* Corresponding Author – boppart@illinois.edu.

The authors declare no conflicts of interest with regard to this work. Additional information can be found at <http://biophotonics.illinois.edu>.

## Introduction

Glucocorticoids remain the most broadly used anti-inflammatory drugs in clinical practice (1). Since the introduction of topical hydrocortisone in the early 1950s, these drugs have been used for localized treatment of inflammatory skin disorders such as eczema and psoriasis (2). However, there are many adverse side effects caused by topical steroid treatment, often associated with skin atrophy. Skin atrophy is characterized by a loss of the barrier function which can result in increased permeability and transepidermal water loss (3). In addition, the atrophied area is much more fragile and has greater potential for tearing, bruising, and infection. In treatment regimens utilizing superpotent steroids, these effects can be quite severe and are potentially irreversible (1).

Histological analysis of topical skin steroid treatment in humans and in animal models has found a decrease in the number of keratinocytes and fibroblasts (4), a decrease in the size of keratinocytes (5), reduced epidermal thickness (6), and a relatively flat dermal-epidermal junction (7) compared to untreated skin. Topical steroids have also been shown to decrease the proliferation rates of keratinocytes and fibroblasts (8, 9) as well as accelerate the maturation of these cells (10). A decrease in Type I collagen production by dermal fibroblasts has also been observed (11). This results in a reorganization of the collagen fibers in which dense, compact bundles are formed in place of the more structurally sound “basketweave” meshwork (12). Even with these observations, the exact mechanism responsible for these adverse effects due to topical steroid treatment remains elusive (13).

Current methods that exist for assessing the skin atrophy potential *in vivo* in humans or animal models include x-ray (14) and ultrasound (4) measurements of skin thickness, as well as dermoscopic observation of the skin surface (15). For x-ray and ultrasound measurements, only structural thickness changes may be observed with low resolution, and the progression of functional changes such as cellular metabolism cannot be measured. Dermoscopic observations provide only magnified photographs of the skin surface, ignoring the important depth-dependent information needed to assess early changes associated with skin atrophy. New optical microscopy methods for the evaluation of the atrophogenic potential of topical corticosteroids have been developed to enable noninvasive probing of the structural and functional properties of the skin microenvironment in an effort to better understand, observe, and track adverse reactions to topical steroid treatment in skin. Laser scanning confocal microscopy (LSCM) has allowed the visualization of keratinocytes *in vivo*, allowing changes in cell size to be observed in human patients (4). More recently, multiphoton microscopy (MPM) has been used to distinguish keratinocytes and collagen in the skin, allowing both visualization of the skin cell layers and measurements of skin thickness (16). However, in these studies, only structural information about the skin thickness and cell layers was obtained and any molecular or functional changes were largely ignored.

In the present study, functional parameters regarding epidermal cell metabolism and structural measures of dermal collagen in the corticosteroid-treated skin microenvironment are measured simultaneously using a multimodal optical microscope. While in previous

studies, the focus was mainly on identifying structural changes within epidermal keratinocytes (4, 16), the focus here is to instead study the metabolic environment of epidermal keratinocytes which may precede epidermal thinning. With this imaging system, subtle changes resulting from steroid treatment are observed that cannot otherwise be detected with LSCM or MPM alone. This multimodal microscope allows for the simultaneous acquisition of images utilizing two-photon excited fluorescence (TPEF), second harmonic generation (SHG), and fluorescence lifetime imaging microscopy (FLIM). TPEF is a nonlinear fluorescence imaging technique in which exogenous or endogenous fluorophores are excited with the simultaneous absorption of two photons (17). SHG is a nonlinear imaging technique highly sensitive to noncentrosymmetric crystalline structure (18). FLIM is an additive detection scheme to TPEF imaging in which the lifetime of the fluorescence emitted from the fluorophores is measured, allowing sensitive quantification of metabolism (19), pH (20), local oxygen and calcium concentrations (21, 22), as well as other important biological parameters. Previously, this multimodal microscope has been used to assess and quantify wound healing parameters (23, 24), to investigate cell death processes (25), and to evaluate human engineered skin constructs (26). In this study, TPEF and FLIM are used to follow the structural and metabolic changes of keratinocytes and SHG is used to identify alterations in the organization and structure of collagen networks following treatment with fluticasone propionate (FP) (27) and mometasone furoate (MF) (28). For the steroids used in this study, FP is a class 5 topical steroid and MF, which is slightly more potent, is listed as a class 4 topical steroid.

## Methods

### Study design

In this study, a hairless mouse model (SKH1-Elite, Charles River) of topical steroid-induced skin atrophy was used to investigate the longitudinal structural and functional alterations in the skin microenvironment. This model has been used previously to study the effects of steroid-induced atrophy (29). Fifteen mice were separated into three groups of five mice each. One group was untreated while the other two groups were treated with either FP (0.05% cream, Fougera, class 5 topical steroid) or MF (0.1% cream, Merck Elocon, class 4 topical steroid). Steroid treated animals were imaged on days 1, 3, 7, 14, and 21. The untreated control group was imaged on days 1, 7, 14, and 21. After each imaging session, one animal was removed from the study and a skin sample was excised from the area of the imaging site for direct histological comparison of longitudinal changes. All studies were conducted under a protocol approved by the University of Illinois at Urbana-Champaign Institutional Animal Care and Use Committee (IACUC) and the GlaxoSmithKline Policy on the Care, Welfare and Treatment of Laboratory Animals.

### Integrated multimodal optical microscope

A custom-built multimodal optical microscope was used to perform the imaging (Figure S1). The unique combination of TPEF, SHG, and FLIM can provide both structural and functional information regarding the skin microenvironment with cellular resolution. Excitation light was provided by a titanium:sapphire laser (MaiTai HP, Spectra Physics) centered at a wavelength of 730 nm, which is focused beneath the skin using a high

numerical aperture (NA) objective lens (XLUMP20X, Olympus). The optical power at the focus was less than seven milliwatts. The focal spot was raster scanned transversely across the sample using a pair of computer-controlled galvanometric mirrors (Micromax 671, Cambridge Technology). Detection of fluorescence and SHG was performed using a 16 channel photomultiplier tube (PMT) spectrometer (PML-16-C, Becker-Hickl) centered at 450 nm, allowing clear spectral separation of the collected SHG and fluorescence photons. In order to obtain fluorescence lifetime curves, time-correlated single photon counting (TCSPC) was performed using a commercial TCSPC data acquisition board (SPC-150, Becker-Hickl). For FLIM imaging, data were acquired from approximately the second keratinocyte layer in the epidermis. For SHG imaging, a stack of images spanning the superficial dermis was acquired for each animal. Data analysis was performed for TPEF and SHG images using both Matlab (MathWorks, R2014a) and ImageJ (National Institutes of Health, v. 1.47m), while FLIM analysis was performed using SPCImage (Becker-Hickl, v. 3.0.8.0).

### Statistical analysis of NADH fluorescence lifetime images

In order to directly compare the *in vivo* response of the three experimental groups, statistical analysis of the cellular response at each imaging time point was performed. It is well established *in vivo* in skin that the metabolism of epidermal keratinocytes have an appreciable depth dependence (30) leading to a depth-dependent response of the mean fluorescence lifetime of NADH as well. Therefore, it is quite important to compare measurements across cellular regions from the images which contain cells of approximately the same size. However, as the skin of the mice used in these experiments is approximately 10-15  $\mu\text{m}$  thick and only a few cell layers are present in the epidermis (29), it can be quite difficult to acquire data from cellular regions of approximately the same size. Therefore in order to accurately compare the data across each experimental groups, regions of interest containing patches of cells from approximately the second layer were manually selected for analysis. This also removes the effect of folds and artifacts clearly present in the skin as seen in Figures 1 and 2. The fluorescence lifetime values from these regions of interest were ultimately used to directly compare the effects of the different treatments to control measurements using the Student's t-test.

### Quantification of local collagen alignment and density

Local collagen alignment was assessed quantitatively using the 2D spatial Fourier transform of local image patches or regions-of-interest. Collagen alignment has been assessed previously on a more global scale through the use of the 2D Fourier transform of the entire acquired SHG image (31). The orientation index, a metric for describing the relative degree of orientation, was described by finding the aspect ratio of the fitted ellipse to a binarized mask obtained from the magnitude of the 2D Fourier transform of the image (31). The orientation index is calculated as

$$N = 1 - \left( \frac{\text{minor Axis}}{\text{major Axis}} \right).$$

This metric takes on values between zero and one where larger values represent more aligned collagen networks. These Fourier transform techniques have been used to accurately quantify both the degree and direction of collagen alignment (32, 33). Matlab (MathWorks, R2014a) was used to calculate the orientation index of local regions-of-interest (ROI) in each SHG image. To begin, several ROIs of pixel length  $40 \times 40$  were selected from each SHG image for local analysis. The orientation index was calculated as above, and for the entire set of images, the mean local orientation index was calculated to identify the degree of local collagen orientation. Density analysis was performed using a fill fraction metric calculated by counting the number of pixels in each ROI with intensity values greater than the mean intensity of the particular image ROI.

### **Histological preparation and analysis**

After resection of skin samples following imaging, samples were fixed in 10% formalin and paraffin embedded. After embedding, tissue specimens were sectioned (at  $5 \mu\text{m}$  thickness) and stained both for hematoxylin and eosin (H&E) and Masson's Trichrome. After staining, a commercial slide scanner (Nanozoomer, Hamamatsu) was used to digitally scan the slides. Images were analyzed with the assistance of a board certified veterinary anatomic pathologist utilizing the commercial visualization software provided (OlyVIA 2.6, Olympus).

## **Results**

### **Multimodal imaging of in vivo skin following steroid treatment**

TPEF, FLIM, and SHG imaging were performed in order to visualize the local skin area affected by topical corticosteroid treatment. TPEF images allow visualization of keratinocyte structure (Figure S2a), the SHG images show the collagen structure in the dermis (Figure S2b), and the FLIM images are used to quantify the relative concentration of free and protein-bound NADH (Figure S2c).

### **Longitudinal tracking of metabolic activity in steroid treated skin**

FLIM was utilized to track the effects of topical steroid application on relative NADH concentrations in order to assess biochemical and molecular intracellular alterations following steroid treatment. Untreated (Figure S3), as well as FP treated (Figure 1) and MF treated (Figure 2) animals were imaged at each time point. A shift toward longer fluorescence lifetime can be clearly observed in FP treated animals at day 21 (Figure 1e) and in MF treated animals at day 14 (Figure 2d) and day 21 (Figure 2e). These shifts in the lifetime can be clearly observed in mean lifetime histograms of the FP (Figure 1f) and MF (Figure 2f) groups when compared to untreated animals (Figure S3e). Quantifying the mean lifetime from several skin locations across each group shows a significant increase in fluorescence lifetime in the FP treated group at day 21 and in the MF treated group at days 14 and 21 (Figure 3).

### **Longitudinal tracking of collagen reorganization in steroid treated skin**

Collagen organization and orientation were visualized using SHG imaging of the dermal layers of the skin. Upon analysis of the acquired images, the organization of dermal collagen

was seen to change with both FP and MF treatment. Dense deposits of Type I collagen were observed at later time points for FP (Figure 4b, red ellipse) and MF (Figure 4c, red ellipse) with strong local alignment when compared to the “basketweave” appearance seen in untreated animals (Figure 4a). Quantification of local alignment and density was performed using a localized orientation index based on the two-dimensional spatial Fourier transform of small image blocks as well as a measurement of the fill fraction of pixels with appreciable signal in each image block. These analyses revealed significant increases in the local collagen alignment of FP treated group at days 14 and 21 and MF treated group at day 21 (Figure 4d) as well as a significant increase in the fill fraction in the FP treated group at day 14 and in MF treated groups at day 21 (Figure 4e).

### Comparison of results with histology

At various imaging time points, imaged areas of the skin were excised and prepared for histological assessment. Tissues were sectioned and stained with hematoxylin and eosin (H&E) in order to assess the structural alterations of the dermal and epidermal skin layers, and with Masson’s trichrome stain to further evaluate the structural properties of the connective tissue in the dermis. Skin thickness changes in hairless mice are typically difficult to assess due to the fact that the normal skin epidermis is only a few cell layers thick and the loss of only a few cell layers can be difficult to quantify (29). Therefore it is difficult to determine any structural effects of epidermal atrophy from H&E stained tissue sections for FP (Figure S4b) and MF (Figure S4c) groups compared to the untreated group (Figure S4a). Blue stained collagen, readily identifiable by Masson’s trichrome staining, appeared prominent within the dermis for FP (Figure S4b) and MF (Figure S4c) treated groups compared to the untreated group (Figure S4a) at day 21. This prominent appearance in FP and MF treated groups likely correlates with the SHG imaging findings.

### Discussion

This study presents quantitative findings of the structural and functional alterations of the epidermal and dermal skin microenvironment following treatment with clinically used topical steroids in a dermatological mouse model (29). Results show that structural features identified with traditional histopathological analysis can be identified *in vivo* through noninvasive imaging, and tracked longitudinally over time in the same animals. This approach has the potential to significantly reduce the time needed for topical drug efficacy evaluation and may be performed clinically using human subjects. Additionally, functional information related to cell metabolism that was collected and quantified cannot be easily observed with traditional histopathology techniques. For both steroid treated groups, changes in dermal collagen organization and NADH mean lifetime in epidermal keratinocytes were observed by day 21, suggesting that multimodal optical microscopy may be a useful tool for monitoring and tracking longitudinally the effects of topical steroids.

Epidermal atrophy and thinning due to topical corticosteroid treatment has been characterized previously, and increased rates of cell differentiation without a corresponding increase in cell proliferation rates were identified (10). Thus, keratinocytes were observed to mature at faster rates, differentiating to corneocytes and ultimately being shed off before



beneficial for diagnostic purposes in order to more accurately predict the atrophogenic potential in human patients for which topical corticosteroids must be prescribed.

## Supplementary Material

Refer to Web version on PubMed Central for supplementary material.

## Acknowledgements

We thank Darold Spillman for assistance with logistical and information technology support and Jean-Phillipe Therrien for assistance with the animal model and topical steroid supplies. This research was supported by a sponsored research agreement from GlaxoSmithKline. In this study, A.J.B., Z.A., and Y.Z. performed the research. A.J.B., Z.A., Y.Z., J.L., M.M., and A.H. analyzed the data. E.J.C. assisted with animal care and steroid application. Z.A. and S.A.B. designed the experimental study. A.J.B. was supported by the National Science Foundation Graduate Research Fellowship Program (DGE-1144245). J.L. was supported by the NIH National Cancer Institute Alliance for Nanotechnology in Cancer program (Midwest Cancer Nanotechnology Training Center; R25 CA154015A) and a Support for Under-Represented Groups in Engineering (SURGE) Fellowship (University of Illinois at Urbana-Champaign).

## References

1. Schoepe S, Schäcke H, May E, et al. Glucocorticoid therapy-induced skin atrophy. *Exp Dermatol*. 2006; 15:406–420. [PubMed: 16689857]
2. Katz HI, Hien NT, Praver SE, et al. Superpotent topical steroid treatment of psoriasis vulgaris—clinical efficacy and adrenal function. *J Am Acad Derm*. 1987; 16:804–811. [PubMed: 3553247]
3. Kato JS, Fluhr JW, Man MQ, et al. Short-term glucocorticoid treatment compromises both permeability barrier homeostasis and stratum corneum integrity: Inhibition of epidermal lipid synthesis accounts for functional abnormalities. *J Invest Dermatol*. 2003; 120:456–464. [PubMed: 12603860]
4. Kolbe L, Kligman AM, Schreiner V, et al. Corticosteroid-induced atrophy and barrier impairment measured by non-invasive methods in human skin. *Skin Res Technol*. 2001; 7:73–77. [PubMed: 11393207]
5. Saarni H, Hopsuhavu VK. Decrease of hyaluronate synthesis by anti-inflammatory steroids *in vitro*. *Brit J Dermatol*. 1978; 98:445–449. [PubMed: 638050]
6. Delforno C, Holt PJA, Marks R. Corticosteroid effect on epidermal-cell size. *Brit J Dermatol*. 1978; 98:619–623. [PubMed: 678451]
7. Kimura T, Doi K. Dorsal skin reactions of hairless dogs to topical treatment with corticosteroids. *Toxicol Pathol*. 1999; 27:528–535. [PubMed: 10528632]
8. Fisher LB, Maibach HI. The effect of corticosteroids on human epidermal mitotic activity. *Arch Dermatol*. 1971; 103:39–44. [PubMed: 4321801]
9. Zendejui JG, Inman WH, Carpenter G. Modulation of the mitogenic response of an epidermal growth factor-dependent keratinocyte cell line by dexamethasone, insulin, and transforming growth factor-beta. *J Cell Physiol*. 1988; 136:257–265. [PubMed: 2457593]
10. Laurence EB, Christophers E. Selective action of hydrocortisone on postmitotic epidermal cells *in vivo*. *J Invest Dermatol*. 1976; 66:222–229. [PubMed: 1270832]
11. Nuutinen P, Autio P, Hurskainen T, et al. Glucocorticoid action on skin collagen: overview on clinical significance and consequences. *J Eur Acad Dermatol*. 2001; 15:361–362.
12. Lehmann P, Zheng P, Lavker RM, et al. Corticosteroid atrophy in human-skin - a study by light, scanning, and transmission electron-microscopy. *J Invest Dermatol*. 1983; 81:169–176. [PubMed: 6875302]
13. Schacke H, Docke WD, Asadullah K. Mechanisms involved in the side effects of glucocorticoids. *Pharmacol Therapeut*. 2002; 96:23–43.
14. Marks R, Dykes PJ, Roberts E. The measurement of corticosteroid induced dermal atrophy by a radiological method. *Arch Derm Res*. 1975; 253:93–96.



15. Vazquez-Lopez F, Marghoob AA. Dermoscopic assessment of long-term topical therapies with potent steroids in chronic psoriasis. *J Am Acad Dermatol.* 2004; 51:811–813. [PubMed: 15523365]
16. El Madani HA, Tancrede-Bohin E, Bensussan A, et al. *In vivo* multiphoton imaging of human skin: assessment of topical corticosteroid-induced epidermis atrophy and depigmentation. *J Biomed Opt.* 2012; 17:0260091–0260098.
17. Denk W, Strickler JH, Webb WW. Two-photon laser scanning fluorescence microscopy. *Science.* 1990; 248:73–76. [PubMed: 2321027]
18. Campagnola PJ, Millard AC, Terasaki M, et al. Three-dimensional high-resolution second-harmonic generation imaging of endogenous structural proteins in biological tissues. *Biophys J.* 2002; 82:493–508. [PubMed: 11751336]
19. Skala MC, Riching KM, Gendron-Fitzpatrick A, et al. *In vivo* multiphoton microscopy of NADH and FAD redox states, fluorescence lifetimes, and cellular morphology in precancerous epithelia. *P Natl Acad Sci USA.* 2007; 104:19494–19499.
20. Lin HJ, Herman P, Lakowicz JR. Fluorescence lifetime-resolved pH imaging of living cells. *Cytometry Part A.* 2003; 52:77–89.
21. Agronskaia AV, Tertoolen L, Gerritsen HC. Fast fluorescence lifetime imaging of calcium in living cells. *J Biomed Opt.* 2004; 9:1230–1237. [PubMed: 15568944]
22. Zhong W, Urayama P, Mycek MA. Imaging fluorescence lifetime modulation of a ruthenium-based dye in living cells: the potential for oxygen sensing. *J Phys D Appl Phys.* 2003; 36:1689–1695.
23. Graf BW, Bower AJ, Chaney EJ, et al. *In vivo* multimodal microscopy for detecting bone-marrow-derived cell contribution to skin regeneration. *J Biophotonics.* 2014; 7:96–102. [PubMed: 23401460]
24. Graf BW, Chaney EJ, Marjanovic M, et al. Long-term time-lapse multimodal intravital imaging of regeneration and bone-marrow-derived cell dynamics in skin. *Technology.* 2013; 1:8–19. [PubMed: 25089085]
25. Zhao Y, Marjanovic M, Chaney EJ, et al. Longitudinal label-free tracking of cell death dynamics in living engineered human skin tissue with a multimodal microscope. *Biomed Opt Express.* 2014; 5:3699–3716. [PubMed: 25360383]
26. Zhao Y, Graf BW, Chaney EJ, et al. Integrated multimodal optical microscopy for structural and functional imaging of engineered and natural skin. *J Biophotonics.* 2012; 5:437–448. [PubMed: 22371330]
27. Berth-Jones J, Damstra RJ, Golsch S, et al. Twice weekly fluticasone propionate added to emollient maintenance treatment to reduce risk of relapse in atopic dermatitis: randomised, double blind, parallel group study. *BMJ.* 2003; 326:1367. [PubMed: 12816824]
28. Veien N, Ølholm Larsen P, Thestrup-Pedersen K, et al. Long-term, intermittent treatment of chronic hand eczema with mometasone furoate. *Brit J Dermatol.* 1999; 140:882–886. [PubMed: 10354026]
29. Woodbury R, Kligman AM. The hairless mouse model for assaying the atrophogenicity of topical corticosteroids. *Acta Derm Venereol.* 1992; 72:403–406. [PubMed: 1362829]
30. Balu M, Mazhar A, Hayakawa CK, et al. *In vivo* multiphoton NADH fluorescence reveals depth-dependent keratinocyte metabolism in human skin. *Biophys J.* 2013; 104:258–267. [PubMed: 23332078]
31. Wu SL, Li H, Yang HQ, et al. Quantitative analysis on collagen morphology in aging skin based on multiphoton microscopy. *J Biomed Opt.* 2011; 16:040502. [PubMed: 21529064]
32. Osman OS, Selway JL, Harikumar PE, et al. A novel method to assess collagen architecture in skin. *BMC Bioinformatics.* 2013; 14:260. [PubMed: 23971965]
33. Sivaguru M, Durgam S, Ambekar R, et al. Quantitative analysis of collagen fiber organization in injured tendons using Fourier transform-second harmonic generation imaging. *Opt Express.* 2010; 18:24983–24993. [PubMed: 21164843]
34. Stringari C, Edwards RA, Pate KT, et al. Metabolic trajectory of cellular differentiation in small intestine by phasor fluorescence lifetime microscopy of NADH. *Sci Rep.* 2012; 2.

35. Shetty PK, Galeffi F, Turner DA. Nicotinamide pre-treatment ameliorates NAD (H) hyperoxidation and improves neuronal function after severe hypoxia. *Neurobiol Dis.* 2014; 62:469–478. [PubMed: 24184921]
36. König K. Clinical multiphoton tomography. *J Biophotonics.* 2008; 1:13–23. [PubMed: 19343631]

Author Manuscript

Author Manuscript

Author Manuscript

Author Manuscript

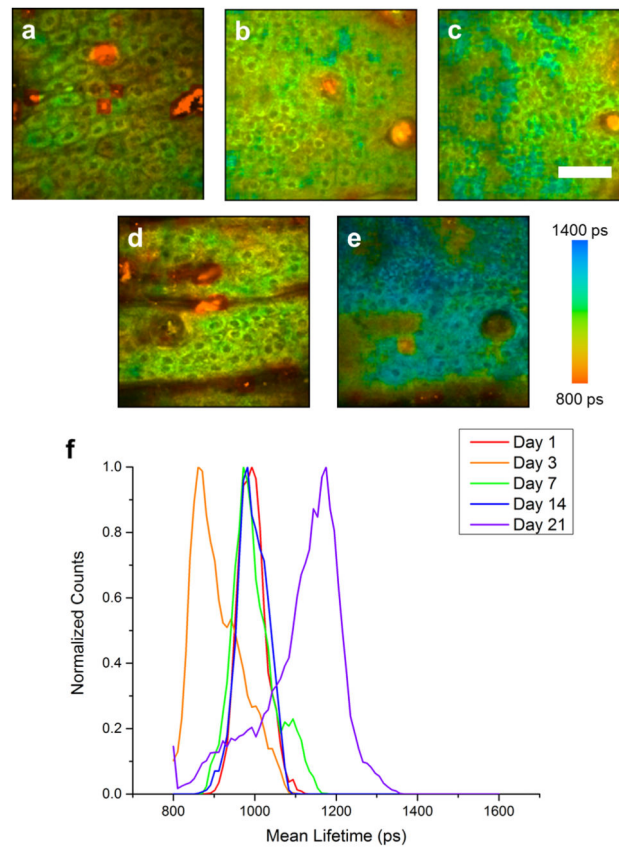


**Figure 1. Longitudinal FLIM imaging of fluticasone propionate (FP) treated animals**  
 Lifetime imaging of keratinocytes in the epidermis at days 1 (a), 3 (b), 7 (c), 14 (d), and 21 (e) in an animal treated twice daily with FP. Normalized histograms of mean NADH lifetime of cell regions show a noticeable increase in mean lifetime at day 21 (f). Scale bar is 50  $\mu\text{m}$ . ps – picoseconds.

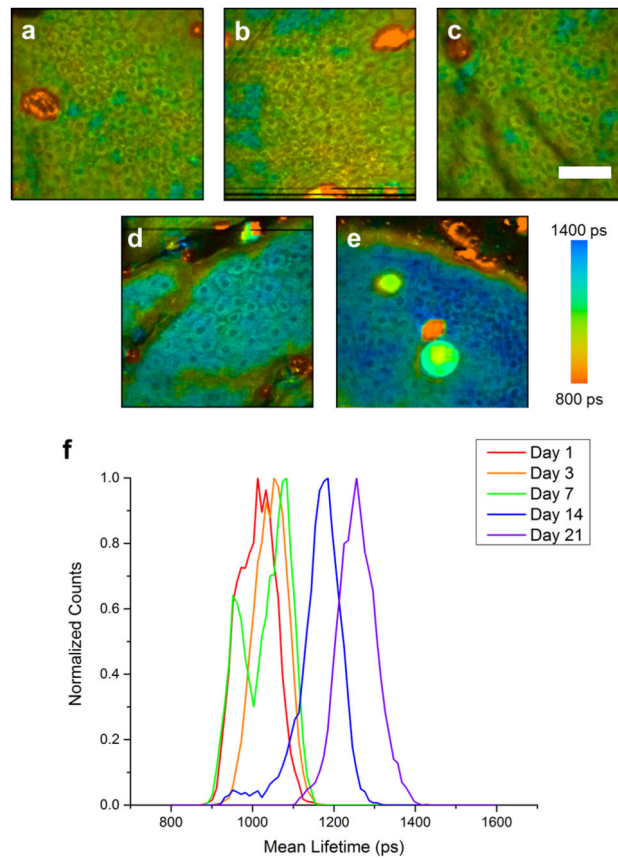


**Figure 2. Longitudinal FLIM imaging of mometasone furoate (MF) treated animals**  
 Lifetime imaging of keratinocytes in the epidermis at days 1 (a), 3 (b), 7 (c), 14 (d), and 21 (e) in an animal treated twice daily with MF. Normalized histograms of mean NADH lifetime of cell regions show a noticeable increase in mean lifetime at days 14 and 21 (f). Scale bar is 50  $\mu\text{m}$ . ps – picoseconds.

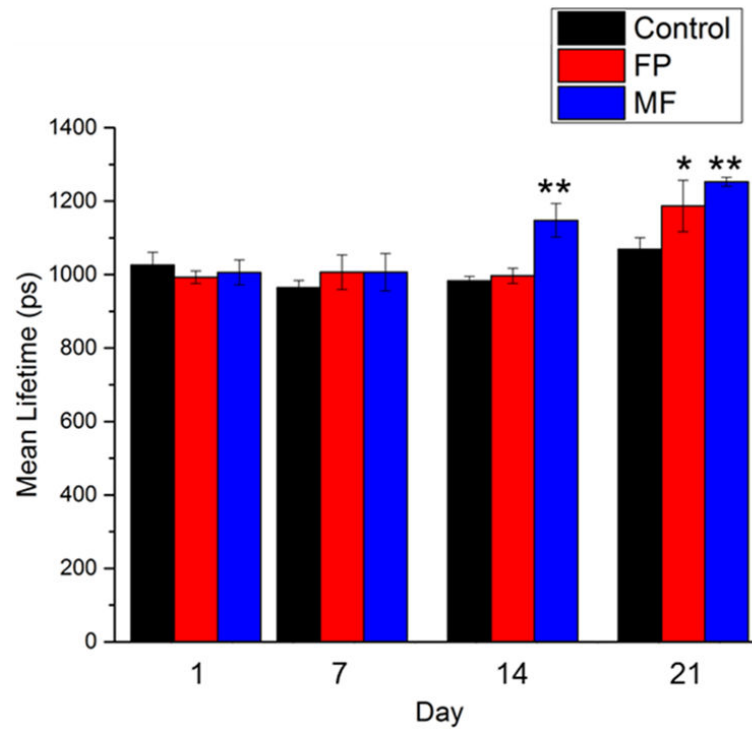


**Figure 3. Statistical analysis of mean NADH lifetime measurements**

Statistical analysis performed on all animals and imaging locations shows a significant increase in mean lifetime for the FP group at day 21 and for the MF group at days 14 and 21 compared to the control group. Statistical testing performed using Student's t-test \*  $p < 0.05$  ; \*\*  $p < 0.01$ .

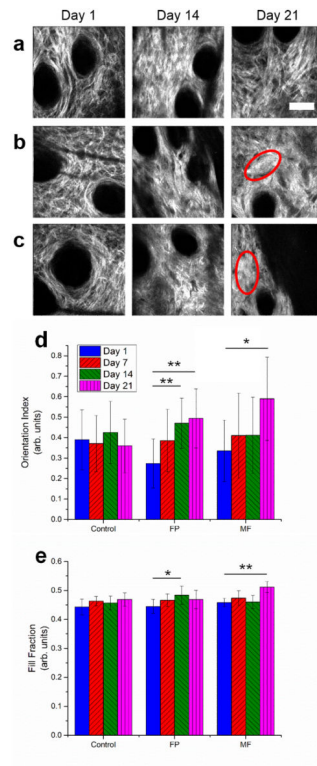


**Figure 4. Analysis of dermal collagen reorganization using SHG imaging metrics**  
 SHG images of dermal collagen in untreated (a), FP (b), and MF (c), groups at days 1, 14, and 21 show the reorganization of collagen networks following topical steroid treatment. At 14 and 21 days following treatment, the collagen networks of FP and MF groups are observed to become denser and locally aligned (red ellipses). Further analysis to quantify the local orientation index and SHG fill fraction revealed a significant increase in the local orientation index (d) and fill fraction (e) of FP and MF treated groups at day 21 using the Student's t-test. Scale bar is 50  $\mu$ m. \*  $p < 0.05$ ; \*\*  $p < 0.01$ .